Observation of ultrahigh-energy electrons by resonance absorption of high-power microwaves in a pulsed plasma

Chirag Rajyaguru, Toshiyuki Fuji,* Hiroaki Ito, Noboru Yugami, and Yasushi Nishida
Energy and Enviromental Science, Graduate School of Engineering, Utsunomiya University, 7-1-2 Yoto, Utsunomiya Tochigi 321-8585, Japan
(Received 8 December 2000; published 15 June 2001)

The interaction of high power microwave with collisionless unmagnetized plasma is studied. Investigation on the generation of superthermal electrons near the critical layer, by the resonance absorption phenomenon, is extended to very high microwave power levels ($\eta = E_0^2/4\pi n_e k T_e \approx 0.3$). Here E_0, n_e, and T_e are the vacuum electric field, electron density, and electron temperature, respectively. Successive generation of electron bunches having maximum energy of about 2 keV, due to nonlinear wave breaking, is observed. The electron energy ϵ scales as a function of the incident microwave power P, according to $\epsilon \propto P^{0.5}$ up to 250 kW. The two-dimensional spatial distribution of high energy electrons reveals that they are generated near the critical layer. However, the lower energy component is again produced in the subcritical density region indicating the possibility of other electron heating mechanisms.

DOI: 10.1103/PhysRevE.64.016403 PACS number(s): 52.35.Mw

I. INTRODUCTION

Absorption of an electromagnetic wave incident on inhomogeneous plasma is important to understand the laser light absorption by plasmas for the design of laser fusion system [1], heat the magnetized fusion plasma, and in problems related to electromagnetic wave propagation in space. The classical inverse bremsstrahlung, for example, becomes inefficient in a hot plamsa due to rapid decrease of the electron-ion collision frequency with temperature and therefore absorption of an intense radiation is then determined by collective effects in the plasma.

When an electromagnetic wave, whose electric field vector is polarized in the plane of incidence, is obliquely incident on an inhomogeneous plasma layer, the component of the electric field along the density gradient tunnels through the reflection point up to the resonance region, where the local plasma frequency becomes equal to the incident radiation frequency. The amplitude of an enhanced electric field in the resonance region is limited by various processes like the collisional effect [2,3], convection of energy by the plasma wave [4–6], nonlinear effects, such as parametric instability [7–9], and wave breaking [4,10–12].

High energy electrons have been observed in many laboratory experiments using microwaves [4,13] with $\eta = E_0^2/4\pi n_e k T_e \approx 3.5\times 10^{-4} \sim 3\times 10^{-3}$, where E_0, k, n_e, and T_e are the vacuum electric field, Boltzmann constant, electron density, and electron temperature, respectively, and in simulations [14–16]. It has also been seen [18] that despite large variation in η, absorption of the incident radiation is mainly due to the resonance absorption phenomenon. For high incident powers, the wave breaking phenomenon [12] and parametric instability are the most probable phenomena for production of high energy electrons [18]. But, strong density modification, associated with intense incident radiations, enhances the range of incidence angle for which resonance absorption is effective and decreases the effects of parametric decay and oscillating two stream instability [18]. Thus the wave breaking phenomnon has the highest probability to account for the generation of high energy electrons in the case of strong incident radiation.

In the present paper, we present experimental observation of superthermal electrons, generated by high power microwave absorption near critical layer, to demonstrate the validity of the cold wave breaking theory even when $\eta \approx 0.3$. When microwaves, with 250 kW of incident power, are launched into unmagnetized and collisionless plasma, superthermal electrons having energy as high as 1.8 keV are observed near the critical layer. The energy scaling of such electrons with microwave power P is measured and the results are in fairly good agreement with those predicted by the wave breaking theory [12]. The main difference in the present experiment as compared to the earlier ones is that the scaling law of high energy electrons has been verified for higher range of η. The energy of electrons in the present work is much higher than that observed in any of the previous laboratory experiments using microwaves. Also, the spatial distribution and temporal evolution of high energy electrons, which have not been measured until now, show that high energy electrons are successively generated from the critical layer as predicted in earlier simulations [16,17]. After the production of the high energy component near the critical region, the lower energy component, having energy between 300 eV and 1.8 keV in the subcritical density region, is also observed. This reveals the possibility of two different electron acceleration mechanisms acting simulataneously at different spatial locations, which will be discussed in detail later.

The paper is organized as follows: experimental arrangment is described in Sec. II and results in Sec. III. Section IV discusses the results and contains calculations of energy gained by the electrons due to nonlinear wave breaking. Section V concludes the paper.

*Now affiliated with Fujitsu General.

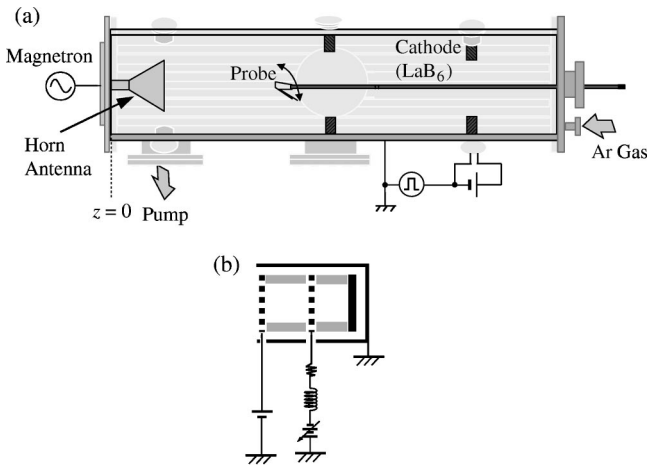

FIG. 1. (a) Experimental setup. (b) Schematic drawing of the energy analyzer.

II. EXPERIMENTAL SETUP

The experimental arrangement is shown schematically in Fig. 1(a). Cylindrical, unmagnetized argon plasma is produced in a stainless-steel chamber of 100 cm length and 32 cm diameter. The outside surface of the vacuum chamber is covered, for improved plasma confinement, with line cusp arrangements, made from permanent magnets having a surface magnetic field strength of 4 kG. Plasma is produced by a pulsed discharge between four LaB_6 cathodes and the grounded chamber wall acting as anode. Typical discharge voltage and discharge duration are 180 V and 1.5 msec, respectively, with the repetition rate of 10 Hz. Typical plasma parameters are $n_e \simeq 2\times10^{12}$ cm^{-3}, $T_e \simeq 2$ eV, and axial density gradient scale-length $L_z \simeq 44$ cm. Argon gas pressure is adjusted to $3\sim5\times10^{-3}$ Torr by a needle valve. Plasma density and temperature are measured by a disk probe with area of 0.96 mm^2, movable along the axis and rotatable in the azimuthal plane. To get better spatial resolution and time response, a disk probe is also used to measure spatial distribution and temporal evolution of high energy electrons. Electrostatic energy analyzer of 23 mm length and 10 mm diameter, capable of measuring electron energy up to 3 keV, is employed for measuring the electron energy distribution function. All three electrodes of the energy analyzer (two grids and one collector) are covered with a copper cup to shield them from microwaves and other noises. The schematic design of shielded energy analyzer is shown in Fig. 1(b). A cylindrical probe with a tip of 1 mm length and 0.25 mm diameter is used to measure the spatial distribution of microwave field. Pulsed microwave has a central frequency, $\omega/2\pi = 9$ GHz (corresponding to cutoff density, $n_c \simeq 1\times10^{12}$ cm^{-3}) and maxmimum power, 250 kW. The pulse duration is variable from 1–3 μs, full width at half maximum (FWHM), with a rise and fall time of 100 ns and a repetition rate of 10 Hz. The present experiment is performed with 1.5 μs. Microwaves are launched into plasma from a rectangular horn antenna, with an aperture area of 14.8×11.7 cm^2. This antenna contains a metal lens for making a ray trace of incident microwave parallel to the propagation direction. Thus the microwave can be considered as a plane wave and this has been confirmed in air without plasma. The antenna is located at the lower end of the plasma density.

III. EXPERIMENTAL RESULTS

When a microwave pulse is injected into the plasma, it is observed that high energy electrons are ejected from the region close to the critical layer. Figure 2(a) shows the typical collector signal of the electrostatic energy analyzer (bottom trace) and wave form of incident microwave (top trace) corresponding to the input power of 100 kW. The first grid of the energy analyser is biased to +30 V, the second grid −500 V, and the collector +100 V. To measure the maximum energy of electrons, the negative bias voltage of the second grid is varied until the collector signal shown in Fig. 2(a) vanishes for the fixed incident microwave power.

Figure 2(b) shows the axial profile of microwave field at $r \simeq 6$ cm (where $r=0$ corresponds to the chamber axis) for three different incident powers and of plasma density in the absence of microwaves. The resonantly excited electric field can be seen at about $z \simeq 44$ cm (where $z=0$ corresponds to that extreme end of the chamber, where the horn antenna is located) clearly, which is the position where the plasma density becomes critical ($\sim1\times10^{12}$ cm^{-3}). Beyond $z \simeq 44$ cm, incident microwaves vanish for all powers as the plasma becomes overdense. It can be seen that electric field at resonance increases in magnitude with the incident power.

In order to investigate the electron energy scaling with incident microwave power, the maximum observed electron energy is plotted as a function of power as shown in Fig. 3. It can be seen very clearly from Fig. 3 that the maximum electron energy ϵ depends on the incident microwave power P as $\epsilon \propto P^{0.47}$. This is in good agreement with that predicted

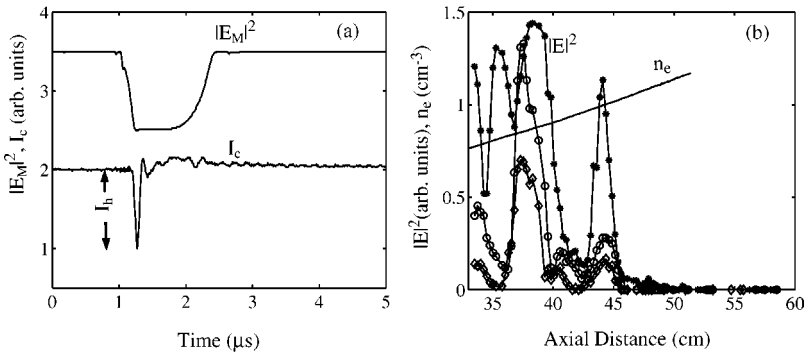

FIG. 2. (a) Typical time history of collector signal from the energy analyzer (bottom) and microwave pulse (top). (b) Axial profile of microwave electric field inside the plasma, using a needle probe, for 250 kw (*), 150 kW (○), 50 kW (◇), and the density profile at $r \simeq 6$ cm (solid line).

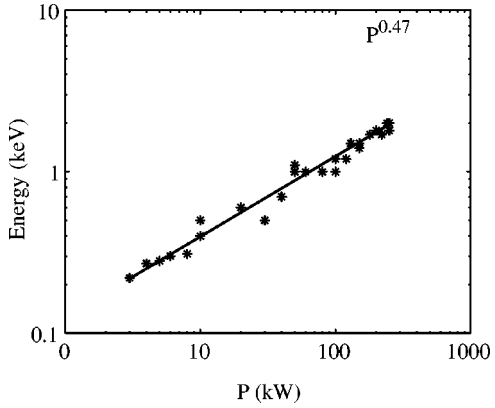

FIG. 3. The highest energy of ejected electrons as a function of incident mirowave power showing the scaling law of high energy electrons.

by the wave breaking theory as $\epsilon \propto P^{0.5}$ [12]. Power dependence and calculations of electron energy for the present experimental parameters will be given later.

For getting better physical insight of mechanisms acting in the resonance region, spatial distribution and temporal evolution of hot electrons are measured and depicted in Fig. 4(a). To measure these results, a one sided disk probe is emloyed with retarding bias of -300 V to collect electrons with energy higher than 300 eV. Two dark spots (where increased darkness corresponds to enhanced flux of high energy electrons) at $r \simeq \pm 6$ cm and $z \simeq 44$ cm, near the critical layer, are clearly showing the locations, where hot electrons are generated. These positions are very close to the resonance region. As the maximum absorption of incident radiation takes place at an optimum angle, the angle of incidence can be unfolded from the above measurements as follows: As hot electrons are observed at $r \simeq \pm 6$ cm and $z \simeq 44$ cm, maximum absorption of microwaves takes place at these locations. Defining z_h to be the microwave launching point, one can obtain the following equation for the angle of incidence:

$$2\cos^2\theta = 1 + \frac{z_h}{L_z} \pm \left[\left(1 - \frac{z_h}{L_z} \right)^2 - \left(\frac{r}{L_z} \right)^2 \right]^{1/2}. \qquad (1)$$

With a measured value of $z_h = 26$ cm, $r = 6$ cm, $L_z = 44$ cm, one obtains $\theta = 49.9°$ and $\theta = 5°$. Out of these two roots, we can neglect $\theta = 49.9°$ as follows. If we assume that the axial profile of the electric field, shown in Fig. 2(b), describes the Airy function pattern, the distance D between the last two peaks of electric field can be written as

$$D = Lz[\sin^2\theta + (k_0 L_z)^{-2/3}]. \qquad (2)$$

If we use Eq. (2) for $\theta = 49.9°$, we get $D \simeq 28$ cm which is much larger than $D \simeq 7$ cm observed in Fig. 2(b). Thus we believe that angle of incidence in the present case is approximately $\theta = 5°$. Determination of the incident angle from Eq. (2) will not be very accurate as it requires the electric field profile to describe the Airy function pattern. This condition will not completely be fulfilled in actual experimental conditions due to reflections of microwaves from chamber walls, radial density gradient, and deviation from linear axial density profile. Also, the angle of incidence depends very sensitively on D for its values close to $(k_0 L_z)^{-2/3}$. Thus small errors in measurement of D can also change the value of the incident angle very much.

Interestingly, another location is also seen around $z \simeq 37$ cm and $r \simeq \pm 6$ cm, where hot electrons are generated. The observation of hot electrons at two different positions, as mentioned above, motivated us to investigate their temporal evolution. Accordingly, the temporal evolution of high energy electrons at $r \simeq 6$ cm is shown in Fig. 4(b). I_h indicates the peak current collected due to hot electrons as indicated in Fig. 2(a). It is clearly observed that hot electron bunches are successively generated near the critical layer ($z \simeq 44$ cm) for all times (40–540 ns) during which incident microwave is present. However, electron flux observed near $z \simeq 37$ cm, is produced at later time (~ 180 ns). It is clear that high energy electrons are produced at different time and spatial locations indicating two different phenomena acting simultaneously in these two regions. The details will be discussed in the next section.

In Fig. 4(b), it appears that high energy electrons near the critical layer disappear after moving a certain distance, but they do not and it can be explained as follows: High energy electrons should move in the direction of density gradient [18,19]. In the present case, the expected direction of acceleration is perpendicular to the density contours starting from the dark spot (origin of high energy electrons) as shown in Fig. 4(a). Presently, the probe in the radial direction cannot be moved, so the distance between the probe tip and the points on the density gradient direction will increase as the probe is moved in the axial direction and hence the probe may completely miss these electrons after the probe is moved away for a ceratin distance in the axial direction. That

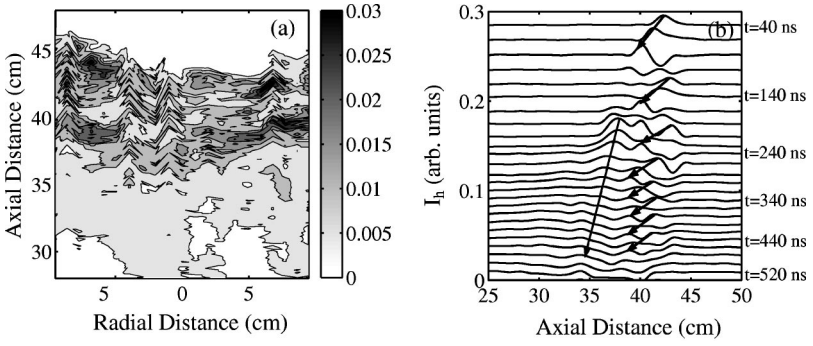

FIG. 4. Spatial distribution and temporal evolution of high energy electrons measured by disk probe, with applied bias voltage of -300 V to collect electrons of energy more than 300 eV. (a) Contour map showing two-dimensional spatial distribution of high energy electrons for an incident power of 250 kW. (b) Temporal evolution of high energy electron bursts at $r \simeq 6$ cm for an incident power of 250 kW.

is why high energy electrons are not collected by probe and seem to disappear in Fig. 4(b). It would be better to measure spatial distribution and temporal evolution of high energy electrons in a full two-dimensional plan to cross check the energy of electrons from the time of flight method by measuring the distance travelled by electrons in a specific time interval. This approach can give the velocity with which electrons are moving and hence their energy.

IV. DISCUSSION

This section discusses foregoing results qualitatively and contains a brief review of various processes occurring in the resonance region. When high power microwaves are launched in inhomogeneous plasma, the component of the electric field parallel to the density gradient tunnels up to the resonance region, where the local plasma frequency approximately equals the incident microwave frequency. The amplitude of the electric field at the resonance region is limited by collisions or energy convection by plasma wave, if the incident power is not high; otherwise the amplitude is limited by resonance breakdown. Parameters $S_{nonl}=(eE_0/m\omega^2L_z)^{1/2}$ and $S_T=(\lambda_D/L_z)^{2/3}$, where λ_D, e, m are the electron Debye length, electron charge, and electron mass, respectively, define the regimes for wave breaking and the plasma wave convection phenomena, respectively, which are responsible for limiting the amplitude of the electric field near the resonance region [16]. If electron temperature does not play an important role and the incident radiation power is high, or mathematically $S_{nonl} \gg S_T$, then whole energy of the wave, after wave breaking, should go to fast electrons. But in the case when $S_{nonl} \geqslant S_T$, the whole energy does not go to fast electrons, but a part of it is carried away by nonlinear plasma waves after the wave breaking [16]. The maximum value of the field at resonance is given by [20]

$$E_{max} \approx E_d/S_{nonl}, \tag{3}$$

where E_d is the high frequency field at resonance connected to E_0 by $E_d=E_0\phi(\tau)/(2\pi k_0 L_z)^{1/2}$, where $\phi(\tau)$ is Ginzburg function. A brief review of wave breaking phenomenon would help form a base for its analytical treatment to see power dependence and the calculation of electron energy. The field at resonance, initially, builds up linearly in time and reaches its maximum value, given by Eq. (3), within a very short time for high incident powers [12]. At the same time, energy conservation in the resonance region requires the contraction of resonance width, within which the field is localized [12]. The wave breaking occurs when the displacement of electrons by the wave electric field in one oscillation period becomes comparable to the dimension of resonance width [20],

$$\Delta x \approx S_{nonl} L_z. \tag{4}$$

At this time resonance breaks down and the energy goes to plasma electrons resulting in the ejection of a high energy electron burst. The velocity of the electrons, at the time of wave breaking, exceeds the velocity of free oscillations due to the driver. In other words, the energy lost by collective oscillations through initial wave breaking exceeds that supplied by the driver field in a period and can represent a significant fraction of total energy in the system. As a result, resonant oscillations start approaching the less energetic state. Similar particle bursts from the resonance region also occur in subsequent periods of oscillations. The field at the resonance then ceases to increase. One may expect that regular electron bursts (through the period) will continue until there is an appreciable energy loss due to the departure of accelerated particles. If these particles leave the plasma, the field amplitude at the resonance reaches again, after a time $\sim \pi/\omega S_{nonl}$, its maximum [16] and therefore a new series of bursts of accelerated particles appears leading to the successive generation of high energy electrons near the resonance as observed in the present experiment. This kind of quasiperiodic behavior has been seen in simulations [15,16].

In order to derive the electron energy scaling law and calculate the maximum electron energy for the present experimental parameters, we recall some analytical aspects of the cold wave breaking theory associated with resonant absorption of a monochromatic pump (frequency ω). Electron displacement in the presence of the externally imposed field is governed by [12,13,21,22]

$$\frac{d^2\delta}{dt^2} + \omega_p^2(z_0)\,\delta = \delta_0\omega^2 e^{i\omega t}, \tag{5}$$

where $\delta_0=eE_d/m\omega^2 \ll L_z$, $\omega_p^2(z_0)=\omega^2(1+z/L_z)$, and $z=z_0+\delta(z_0,t)$ are the electron displacement in the driver, local electron plasma frequency, and spatial coordinate, respectively. Wave breaking occurs when $\partial\delta/\partial z_0=-1$, which yields the electron velocity $(2\omega^2 L_z\delta_0)^{1/2}$ and this results in maximum energy $\epsilon=(1/2)m\langle\dot{\delta}\rangle^2$ given by [12]

$$\epsilon = m\omega^2 L_z \delta_0. \tag{6}$$

Using the definition of δ_0, the above formula reduces to

$$\epsilon = eE_d L_z. \tag{7}$$

Equation (7) can be undertood physically from the fact that, as described earlier also, the conservation of energy in the resonance region requires that an increase in the field amplitude should be exactly balanced by the contraction of resonance width. Thus the energy gained by electrons passing through the resonance region of the width Δx in one oscillation period of the wave can be written as $eE_{wav}\Delta x$. Making use of Eqs. (3) and (4), we again get the result given by Eq. (7). Using the definition of E_d for the optimum angle of incidence, we have from Eq. (7)

$$\epsilon = \frac{1}{2\pi}\frac{eE_0L_z}{\sqrt{L_z/\lambda_0}}. \tag{8}$$

Dividing Eq. (8) by the electron rest mass energy mc^2 and T_e, one gets

$$\frac{\epsilon}{T_e} = \left[\frac{E_0^2}{4\pi n_e T_e}\frac{mc^2}{T_e}\frac{L_z}{\lambda_0}\right]^{1/2}. \tag{9}$$

Using the definition $\eta = E_0^2/4\pi n_e T_e$, Eq. (9) can finally be written as

$$\frac{\epsilon}{T_e} = \eta^{0.5}\left(\frac{mc^2}{T_e}\right)^{1/2}\left(\frac{L_z}{\lambda_0}\right)^{1/2}. \tag{10}$$

Since $\eta \propto P$, from Eq. (10), the maximum energy of electrons ejected due to wave breaking scales as $\epsilon \propto P^{0.5}$ which is confirmed experimentally in the present paper. Substituting the present experimental parameters $\eta \simeq 0.3$, $T_e \simeq 2$ eV, and $mc^2 \simeq 512$ keV, one gets $\epsilon \simeq 2.4$ keV which is in good agreement with the experimentally measured electron energy (see Fig. 3).

Now we will explain the phenomenon responsible for the generation of high energy electrons near the region around $z \simeq 37$ cm in Fig. 4(b). Although the exact mechanism is not very well understood at present, some of the possibilities may be considered. In all previous works, It has been reported that parametric instability is the most prominent candidate to absorb the incident high frequency field after the resonance absorption at high powers [18]. As the incident radiation is intense enough to make $\eta \approx 0.3$, which is well above the theoretically predicted threshold value $\eta_{th} = 6 \times 10^{-3}$ for the parametric instability, its possibility cannot be ignored. But, it requires matching the condition of wave numbers and frequencies between incident microwave and other two parametrically coupled waves, viz. electron plasma wave and ion acoustic wave. Thus parametric instability can occur at a location in underdense plasma, which is different from the resonance region. As the difference between the electron plasma frequency and the ion plasma frequency is very large, the frequency matching condition will require that the plasma wave frequency should be very close to the external pump frequency, which in turn requires the spatial location to be very close to the resonance region on the lower density side. In the present case, however, the expected spatial location, where parametric instability can occur, comes out to be only 1.5 cm down the density gradient from the resonance region. Another set of high energy electrons observed in the present experiment is generated approximately 7 cm away from the resonance layer indicating that some mechanisms, other than the parametric instability, are operating to produce high energy electrons in the subcritical density region. Expected candidates are as follows:

(i) It is quite possible that the strong high frequency electric field near $z \simeq 37$ cm, seen in Fig. 2(b), is not necessarily in the direction of the density gradient, and can excite plasma waves, normally having a broad spectrum in wave number space due to plasma inhomogenity, with lower excitation efficiency (due to mismatching of local plasma frequency and incident radiation frequency). These waves can turbulently heat plasma electrons. Due to the nonresonant heating of electrons, we expect that the energy of electrons observed in the lower density region should be less than that observed near the resonance region (~ 1.8 keV). As the measurements shown in Fig. 4(b) are taken by biasing the probe at -300 V, the energy of the electrons at the lower density region is expected to be in the range 300 eV–1.8 keV.

(ii) We have also observed strong density modifications and caviton [23] generation in the present experiment. Temporal evolution of cavitons and high energy electrons in the lower density plasma shows that cavitons and high energy electrons are almost simultaneously generated near $z \simeq 37$ cm. One would expect the trapped high frequency electric field in the caviton structure to greatly affect the electron energy distribution function [15]. However, the mechanism responsible for the generation of the caviton is not very clear at present. Strong density modifications have been observed [15,24,25] because of additional pressure due to the transverse rf (radio frequency) field. Thus a strong transverse field observed near $z \simeq 37$ cm can play important role in caviton generation.

V. CONCLUSIONS

We have extended the investigation of generation of high energy electrons due to nonlinear interaction of high power microwaves with inhomogeneous plasma to the regime, where the incident microwave power is as high as to make $\eta \approx 0.3$. When microwaves with peak power of 250 kW are launched into inhomogeneous plasma, electrons, having maximum energy 1.8 keV, are generated succesively from near the resonance region. Experimental results show that the maximum energy of electrons scales to the incident power approximately as $\epsilon \propto P^{0.5}$ up to 250 kW, showing the validity of wave breaking theory in such a high power regime. Calculation of maximum electron energy on the basis of the wave breaking model shows good agreement with experimental observations. Spatial distribution and temporal evolution of high energy electrons show that lower energy electrons, but having energy >300 eV, are produced at later time and at different location than the resonance region. Possibilities of some mechanisms operating in the subcritical density region are discussed and these are evidently different than resonance absorption phenomena near the critical layer.

ACKNOWLEDGMENTS

We are deeply indebted to Professor N. Andreev, Institute for High Energy Densities, Russian Academy of Sciences and Professor M. Bakunov for their fruitful discussions. We gratefully acknowledge Professor P. K. Kaw, Institute for Plasma Research, Gandhinagar (India), for his valuable suggestions. This work is partly supported by the Grant-in-Aid for Scientific Research from the Ministry of Education, Science, Sports and Culture of Japan. We are also grateful to the Co-operation Research Center, Utsunomiya University, for partly supporting the present experiments.

[1] J. Nuckolls, L. Wood, R. Thiessen, and G. Zimmerman, Nature (London) **239**, 139 (1972); J.S. Clarke, H.N. Fischer, and R.J. Mason, Phys. Rev. Lett. **30**, 89 (1973).
[2] V.L. Ginzburg, *Propagation of Electromagneric Waves in Plasma* (Gorden and Breach, New York, 1961).
[3] M. Colunga, P. Mora, and R. Pellat, Phys. Fluids **28**, 854 (1985).
[4] A.Y. Lee, Y. Nishida, N.C. Luhmann, Jr., C. Randall, M. Rhodes, and S.P. Obenschain, Phys. Fluids **29**, 3785 (1986).
[5] J.C. Adam, A. Gourdin Servenier, and G. Laval, Phys. Fluids **25**, 376 (1982).
[6] G.J. Morales and Y.C. Lee, Phys. Fluids **20**, 1135 (1977).
[7] K. Nishikawa, J. Phys. Soc. Jpn. **24**, 916 (1968); **24**, 1152 (1968); P.K. Kaw and J. Dawson, Phys. Fluids **12**, 2586 (1969).
[8] K. Mizuno and J.S. DeGroot, Phys. Rev. Lett. **35**, 219 (1975).
[9] H. Dreicer, R. Ellis, and J. Ingraham, Phys. Rev. Lett. **31**, 426 (1973).
[10] J. Dawson, Phys. Rev. **113**, 383 (1959).
[11] T.P. Coffey, Phys. Fluids **14**, 1402 (1971).
[12] J. Arbritton and P. Koch, Phys. Fluids **18**, 1136 (1975).
[13] A.Y. Lee, Y. Nishida, N.C. Luhmann, Jr., S.P. Obenschain, B. Gu, M. Rhodes, J.R. Albritton, and E.A. Williams, Phys. Rev. Lett. **48**, 319 (1982).
[14] D.W. Forslund, J.M. Kindel, K. Lee, E.L. Lindman, and R.L. Morse, Phys. Rev. A **11**, 675 (1975).
[15] L.M. Kovrizhnykh and A.S. Sakharov, Fiz. Plazmy **6**, 150 (1980) [Sov. J. Plasma Phys. **6**, 84 (1980)].
[16] S.V. Bulanov, L.M. Kovrizhnykh, and A.S. Sakharov, Zh. Éksp. Teor. Fiz. **72**, 1809 (1977) [Sov. Phys. JETP **45**, 949 (1977)].
[17] L.M. Kovrizhnykh and A.S. Sakharov, Fiz. Plazmy **5**, 840 (1979) [Sov. J. Plasma Phys. **5**, 470 (1979)].
[18] K.G. Estabrrok, E.L. Valeo, and W.L. Kruer, Phys. Fluids **18**, 1151 (1975).
[19] V.I. Barinov, Fiz. Plazmy **3**, 239 (1997) [Sov. J. Plasma Phys. **3**, 132 (1977)].
[20] S.V. Bulanov and L.M. Kovrizhnykh, Fiz. Plazmy **2**, 105 (1976) [Sov. J. Plasma Phys. **2**, 58 (1976)].
[21] J.P. Freidberg, R.W. Mitchell, R.L. Morse, and L.I. Rudsinski, Phys. Rev. Lett. **28**, 795 (1972).
[22] P. Koch and J.R. Albritton, Phys. Rev. Lett. **32**, 1420 (1974).
[23] H.C. Kim, R.L. Stenzel, and A.Y. Wong, Phys. Rev. Lett. **33**, 886 (1974).
[24] N.E. Andreev and V.P. Silin, Fiz. Plazmy **4**, 908 (1978) [Sov. J. Plasma Phys. **4**, 508 (1978)].
[25] N.E. Andreev, V.P. Silin, and G.L. Stenchikov, JETP Lett. **28**, 494 (1978).